Circulation in the South China Sea in summer of 1998

LIU Yonggang, YUAN Yaochu, SU Jilan & JIANG Jingzhong

Second Institute of Oceanography, State Oceanic Administration (SOA), Hangzhou 310012, China; Key Lab of Ocean Dynamic Processes and Satellite Oceanography, SOA, Hangzhou 310012, China

Abstract Based on the CTD and meteorological data obtained by R/V *Xiangyanghong No.14* in the South China Sea (SCS) in the summer of 1998, both current velocity and volume transport are calculated by using a modified inverse model. Circulation in the SCS is analyzed by combining the calculated results with ADCP data. The following results are obtained. (i) The most important feature of the circulation in the northeastern SCS is that a branch of the Kuroshio intrudes into the SCS with a small volume transport. It flows anticyclonically through the Bashi Strait and towards the southwest off the Taiwan Island, and it does not intrude into the inner SCS. (ii) The northern SCS is dominated mainly by a cyclonic circulation system with two cold eddies. (iii) The central and southwestern SCSs are mainly occupied by anticyclonic circulation systems, including three anticyclonic and one stronger cyclonic eddies. (iv) In the southeastern SCS, there is a large scope of cyclonic circulation extending in the SW-NE direction. (v) There is a "multi-eddy phenomenon" in the SCS, and a larger eddy contains several small eddies. (vi) There is western intensifying of the currents and eddies in the SCS.

Keywords: SCS circulation in summer, multi-eddy phenomenon, modified inverse model.

On the calculations of the currents in the SCS, some researchers[1–5] had used dynamic calculation or β-spiral method[4] to compute the circulation with observational hydrographic data. More scientists resorted to numerical models[6–13]. However, no publication has been found about calculation of the currents in the SCS by an inverse model as yet. What is more, the observational data in some cruises were obtained only within limited local areas in the SCS, such as the northern or northeastern SCS[9], eastern SCS[2], central SCS[4] or southern SCS[3, 5]. Both CTD and ADCP observations covering the whole SCS in one cruise were rarely found.

In this paper, based on the CTD and wind data obtained by R/V *Xiangyanghong No.14* in almost the entire SCS after the onset of the Asian Monsoon (from June 12 to July 6, 1998), the current velocity and volume transport (hereafter VT) are calculated by a modified inverse method. Vessel-mounted ADCP and altimetry data are also used to analyze the currents in the SCS and the distribution of the mesoscale eddies in the SCS. The observed CTD stations, sections and the computation boxes in the modified inverse model are shown in fig. 1.

1 Numerical computation and model parameters

Yuan et al.[14,15] had made the following four important modifications for the previous inverse model: (i) Vertical eddy viscosity term is included in momentum equations, i.e. the flow is non-geostrophic. (ii) Vertical eddy diffusion term is considered in the density equation. (iii) An inequality constraint of heat transfer between the atmosphere and the ocean is imposed. (iv) β-effect is also considered.

Computation boxes are shown in fig. 1. In the computation by the modified inverse model mentioned above, each computation box is divided into five vertical layers with σ_{tp} values of 25.0, 26.5, 27.1 and 27.6 at the four interfaces. Due to lack of detailed wind data, a uniform wind field is assumed and an average wind speed of (4.2 m/s, 182°) is obtained by vector averaging wind data observed at each CTD station during the cruise. The heat inequality constraints are not imposed in this computation for lack of heat exchange rate data in the SCS. Vertical eddy viscosity coefficient A_z and vertical eddy diffusion coefficient K_v are taken to be 100 and 10 cm^2/s, respectively. An optimum reference level (ORL) of 1 800 m is selected according to the empirical search method of Fiadeiro and Veronis[16]. Shallow water correction is made as follows in the determination of the reference level: if the water depth of the station (H) is larger than the ORL, it is taken to be ORL, else it is taken to be H.

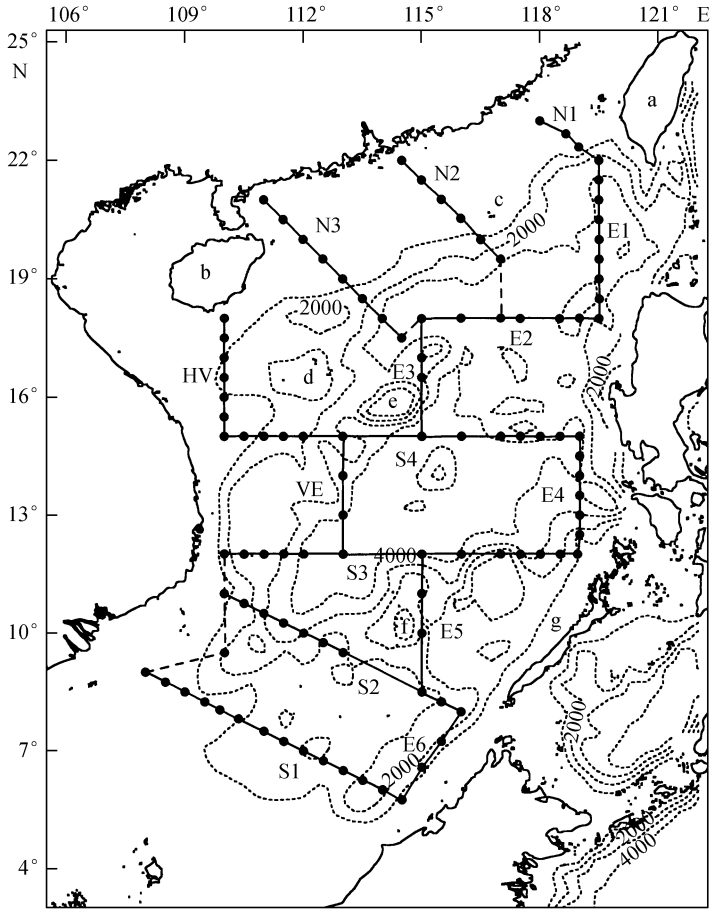

Fig. 1. Topography, observed CTD stations and the sections, and the computation boxes. a, Taiwan Island; b, Hainan Island; c, Dongsha Islands; d, Xisha Islands; e, Zhongsha Islands; f, Nansha Islands; g, Balawan Island.

2 Circulation and eddies in the SCS

In this section, distributions of water temperature are analyzed firstly. Based on the velocity structure and volume transport calculated by the modified inverse model, characteristics of the circulation and eddies in different areas of the SCS are discussed with the layered temperature and ADCP data.

(ⅰ) Horizontal distribution of water temperature. Fig. 2 shows the horizontal distribution of water temperature at 100, 700 and 1 200 m levels in the SCS. In the northeastern SCS, there is a warm water area southwest off Taiwan Island at 100 m level, while a relative cold water area in the central Bashi Strait (fig. 2). However, at both 700 and 1200 m levels, there is an obvious warm eddy south of Dongsha Island.

The northern SCS is mainly dominated by a large scope of cold water (C1) with several cold cores at 100 m level. However, the scope of cold water becomes smaller at 700 m level, with only one cold core at about (116°E, 18°N). When it comes to 1200 m level, the scope of the cold water becomes even smaller, and is almost substituted by two warm eddies.

The central and southwestern SCSs are mainly dominated by warm water at 100 m level, including a warm core near Zhongsha Islands (W1), a warm eddy southeast off Vietnam (W2), a large warm pool (W3) with two warm cores west off the Philippines, and a strong cold eddy (C2) between

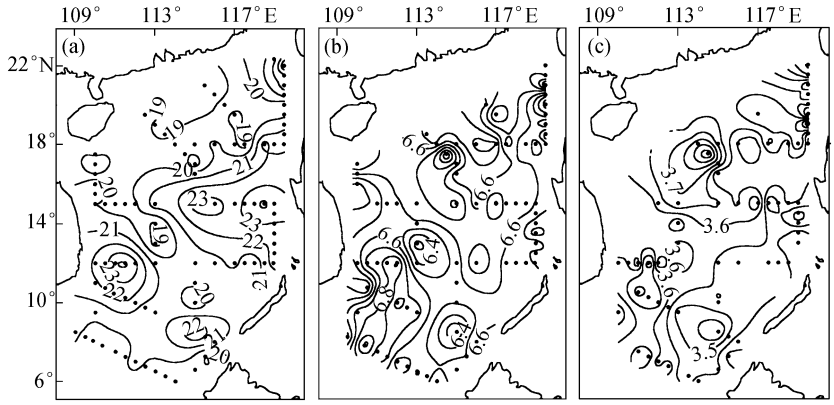

Fig. 2. Horizontal distribution of water temperature at 100 m (a), 700 m (b) and 1 200 m (c) levels.

W2 and W3. In the middle layer (700 m level), the scope of W3 becomes smaller and moves a bit westward, while the scope of W2 becomes larger and extends to Section S1. C2 exists obviously. However, at 1 200 m level, the area west off the Philippines is controlled by cold water, while both the central and southwestern SCSs are dominated by warm water.

In the southeastern SCS, there is a small scope of warm eddy over the Nansha Trough at 100 m level. However, sea water in the area from southwest off the Philippines to the south is relatively cold, with an obvious cold core over the Nansha Trough at 700 m level. In the deep layer at about 1 200 m level, there is a large scope of cold water in the southeastern SCS with a cold core (C3) over the Nansha Trough.

Also, we have computed the geopotential anomaly relative to 1 500 decibar level, and got a circulation pattern in the SCS similar to that from the horizontal temperature distribution (fig. 2). We do not discuss it in detail, due to the limited pages.

In summary, there are several active mesoscale eddies in different layers in the SCS during the observation period, i.e. there is a "multi-eddy phenomenon" in the SCS. From the horizontal distribution of water temperature, it can be seen that the circulation from the surface to 300 m level is quite different from that below 500 m level in the SCS. In the upper layer, the northern SCS is dominated mainly by a cold trough with several cold eddies, and the central and southwestern SCSs are occupied mainly by warm water systems, including three warm water circulation systems and one cold eddy, while in the southern SCS, there is a weak warm eddy over the Nansha Trough. However, in the deep layer below 500 m level, the cold trough in the northern SCS decreases in scope, and is substituted by warm eddies, and the warm eddy west off the Philippines also decreases in scope, but the warm eddy southeast off Vietnam increases in scope. The southeastern SCS is dominated by cold water in the deep layer.

(ii) Velocity distribution. Velocity distribution at each section can be calculated by the modified inverse model. Due to limitation of pages, we will discuss only the velocity distributions at both Section E1 near the Bashi Strait and Section S3 at about 12°N in the central SCS.

Section E1 is in N-S direction (fig. 1). From north to south, eastward and westward currents flow through Section E1 alternately (fig. 3). In the northern end of Section E1, there is an eastward current between computation points 1 and 2 near the Taiwan Island, ranging from the surface to the bottom with a maximum velocity (V_{max}) of 20 cm/s in the subsurface

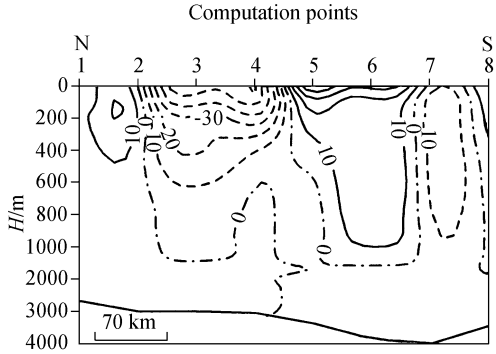

Fig. 3. Velocity distribution at Section E1 (cm/s, positive value: eastward, negative value: westward).

layer. A stronger westward current lies between computation points 3 and 4 with a V_{max} of 61 cm/s at 30 m level of computation point 4. From ADCP current vectors averaged within 25—75 m layer (fig. 4), it seems that a Kuroshio branch east of Luzon flows westward through the Bashi Channel and makes an anticyclonic meander southwest off the Taiwan Island. Moreover, the eastward current between computation points 1 — 2 and the westward current at computation point 3 might compose one part of an anticyclonic eddy southwest of the Taiwan Island (fig. 2(a), (b)). In middle Section E1, both an eastward current at computation point 5 and the westward current at computation point 4 compose one part of a cyclonic circulation in the upper 400 m layers. The eastward current has a V_{max} of 45 cm/s in the surface layer of computation point 5. In the southern part of Section E1, both an eastward current at computation point 6 and a westward current at computation point 7 make up one part of a deep anticyclonic circulation south of Dongsha Islands with its center at about 18°—19°N northwest off the Philippines (fig. 2(b), (c)). Velocities at 1 000 m level of computation points 6 and 7 are greater than 10 cm/s. The westward current at computation point 7 has a V_{max} of 20 cm/s in the subsurface layer. At the southern end of Section E1, there is an eastward current near the coastal Philippines with a V_{max} of 21 cm/s in the surface layer. From fig. 4, it can be seen that calculated velocities are basically in agreement with those measured with ADCP. Some of their small differences can be attributed to effects of tidal currents and local winds.

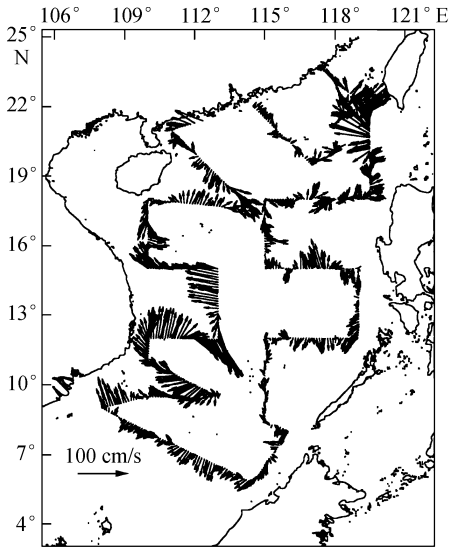

Fig. 4. ADCP currents averaged within the 25—75 m layer.

Section S3 is a latitudinal section at about 12°N. A stronger northward current appears west of computation point 3 near the Vietnam coast with a V_{max} of 56 cm/s in the surface layer of computation point 2 (fig. 5). Between computation points 4 and 5, there is a stronger southward current with a V_{max} of 56 cm/s in the surface layer of computation point 5. Both these two currents compose one part of the stronger anticyclonic eddy (W2) southeast off Vietnam. The eddy W2 can be obviously outlined in ADCP vectors (fig. 4), and it has a warm core with large vertical extent from the upper to the deep layer (fig. 2(a), (b), (c)). Velocities are greater than 10 cm/s at 400 m level of W2. In the middle part of Section S3, there is a weak northward current at computation point 7 with a V_{max} of only 13 cm/s in the surface layer. In the eastern part, there is a southward current at computation point 9 from the surface to the deep layer with a V_{max} of 18 cm/s in the surface layer. Both the weak northward current at computation point 7 and the weak southward current at computation point 6 make up a southern part of the stronger cold eddy (C2) in the central SCS. Also, both the current at computation point 7 and the southward currents at computation point 9 compose one part of the warm eddy (W3) west of the Philippines. To the east, the currents east of computation point 10 are very weak. The calculated results are in good agreement with those measured with ADCP except those at the eastern end of Section S3.

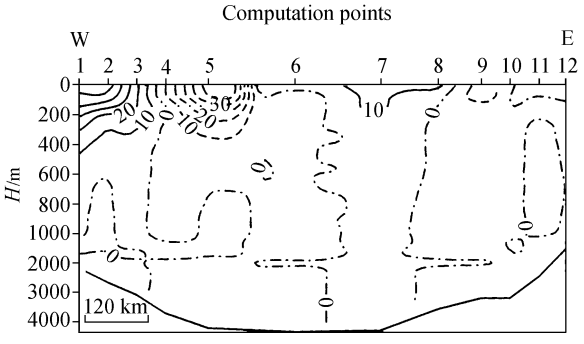

Fig. 5. Velocity distribution at Section S3 (cm/s, positive value: northward, negative value: southward).

From fig. 5, it can be seen that the currents in the western SCS are stronger than

those in the eastern part, which can also be found in ADCP vectors (fig. 4). The stronger currents in the western SCS had also been obtained by numerical modeling[11]. As to its mechanisms, there are different viewpoints. For example, Zeng et al.[6] attributed it to the β-effect, while Chu et al.[10] suggested that the lateral boundary forcing is the major factor for the formation of the strong western boundary currents in the SCS.

(iii) Distribution of stream function and volume transport. In the modified inverse computation, not only should the balance of VT flowing into and out of a computation box be met, but also the balance of VTs through the entire computation area are required. Distribution of stream functions calculated by the modified inverse model is shown in fig. 6. Based on the circulation pattern shown in fig. 6, the following four topics are discussed for the circulation systems in the northeastern SCS, northern SCS, central and southwestern SCS, and southeastern SCS, respectively.

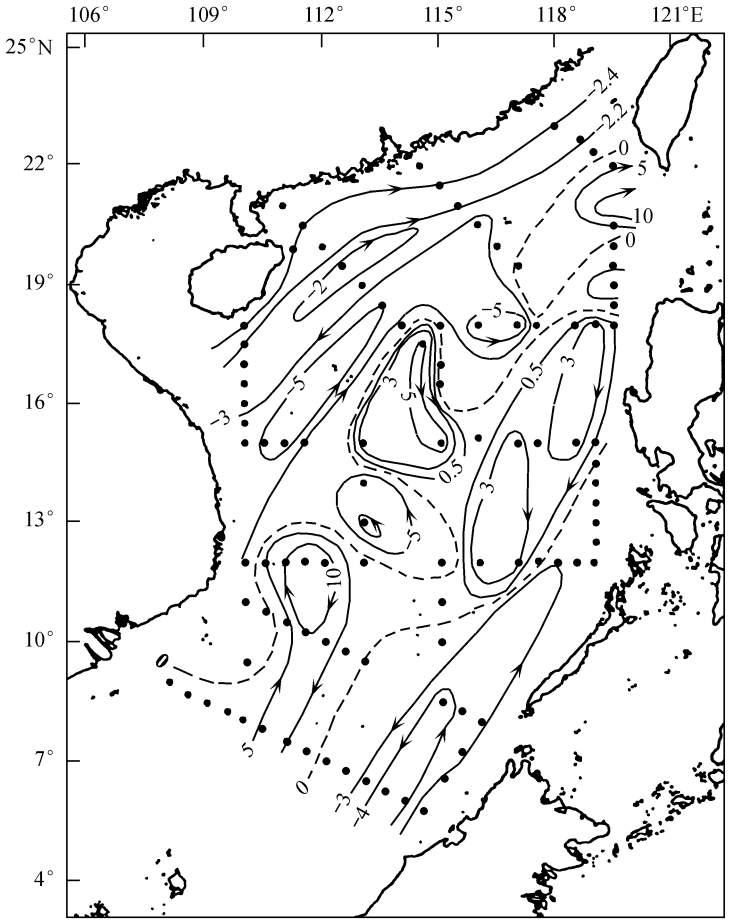

Fig. 6. Distribution of stream function ($10^6 m^3/s$).

(1) Circulation in the northeastern SCS. One of the most important problems about the circulation in the northeastern SCS is whether the Kuroshio branch can intrude into the SCS or not. If yes, how about its circulation pattern? The calculated results show that a branch of the Kuroshio southwest off the Taiwan Island flows into the SCS south of the small anticyclonic eddy through the northern Section E1, and it flows anticyclonically northeastward out of the SCS through the northern Section E1 and Section N1. The branch of the Kuroshio is strong with a V_{max} of 61 cm/s, and the westward VT through Section E1 between computation points 3 and 4 is 16.9×10^6 m^3/s, while the eastward VT between computation points 1 and 2 through the northern Section E1 and Section N1 is

15.7×10^6 m^3/s. It is worthy of note that this value of eastward VT is mainly the sum of the VT values of both the Kuroshio branch and its adjacent anticyclonic eddy. That is to say, after the branch of the Kuroshio passes through the Bashi Channel, its most part flows anticyclonically northeastward out of the SCS south off the Taiwan Island. The Kuroshio branch can intrude into the area west of 118°30′E with the VT of about 5×10^6 m^3/s only, but its intrusion can affect the circulation in an area west most to 117°E and south most to 18°N. This can be attributed to the blocking of the intruding by a cyclonic circulation system in the northern SCS, which will be discussed in the following section. Particularly, the intruding of the Kuroshio branch mentioned above is just one case. In fact, there was no branch of the Kuroshio intruding into the SCS during the strong El Niño in December 1997[17].

(2) Circulation in the northern SCS. The area west of 117°E in the northern SCS is mainly dominated by a cyclonic circulation (C1) system southwest of Dongsha Islands with two cyclonic eddies (fig. 6), and their centers are located at about (116°E, 18°N) and Xisha Islands (112°E, 17°N), respectively. Su et al.[8] discussed the results from layered models, and suggested that advection of vorticity from the Kuroshio front results in a fluctuating cyclonic gyre with migrating cold eddies. As a cyclonic eddy grows, it starts to move westward and continues to grow at the same time. The eddy sheds to the southwest periodically. In this cruise, the cyclonic eddies line up from east to west as cyclone waves in the northern SCS, which seems to be an evidence of Su et al.[8]. As shown in fig. 6, there is a weak northeastward flow along the Guangdong coast, which seems to be the so-called South China Sea Warm Current[18].

The total northeastward and southwestward VTs through Section N2 are 5.6×10^6 and 2.4×10^6 m^3/s, respectively, with a net northeastward VT of 3.2×10^6 m^3/s. The total northeastward and southwestward VTs through Section N3 are 12.3×10^6 and 3.7×10^6 m^3/s, respectively, with a net northeastward VT of 8.6×10^6 m^3/s. South off the Hainan Island, the total eastward and westward VTs through Section HV are 4.2×10^6 and 5.7×10^6 m^3/s, respectively, with a net westward VT of 1.5×10^6 m^3/s.

(3) Circulation in the central and southwestern SCSs. The central and southwestern SCSs are mainly dominated by an anticyclonic circulation system in a SW-NE area indicated by the zero line (dashed) of stream function in fig. 6, including mainly an anticyclonic circulation near Zhongsha Islands (W1), an anticyclonic circulation southeast off Vietnam (W2), and an anticyclonic circulation system west off the Philippines (W3). There is a stronger cyclonic eddy (C2) between W1 and W2. This is a basic structure of the circulation in the central and southwestern SCSs. Such kind of circulation pattern can also be shown from the velocity distribution, ADCP currents and the distribution of water temperature. The circulation systems are discussed as follows. (ⅰ) The anticyclonic circulation W2. It has a large scope including the western parts of Sections S1, S2 and S3, and the area north of Section S3, and its center is located at about (111°30′E, 11°N) (fig. 6). It is very strong with a V_{max} of 56 cm/s and a large VT of about 16×10^6 m^3/s. From temperature distribution, its warm core extends from the surface to the deep layer (fig. 2(a), (b), (c)). (ⅱ) The cyclonic eddy C2. It is located between anticyclonic eddies W1 and W2 with its center at about (113°E, 13°N). It is also strong with a V_{max} of 52 cm/s and a VT of about 12×10^6 m^3/s. The similar flow pattern as mentioned above, i.e. both a northern cyclonic eddy (C2) and a southern anticyclonic eddy (W2) southeast off Vietnam, had been obtained from a numerical simulation with a little south for the locations of both eddies [11]. The similar circulation structure has also been revealed in the upper layer of western SCS with the HAMSOM model[13]. (ⅲ) The anticyclonic circulation W1. W1 is located near the Zhongsha Islands, and it is not stronger than the above two eddies with a VT of about 6×10^6 m^3/s. (ⅳ) The anticyclonic circulation system W3. W3 is located west off the Philippines including two anticyclonic eddies W3-1 and W3-2 in its northeastern and southwestern parts, respectively (fig. 6). Both W3-1 and W3-2 are very weak with VTs of about 6×10^6 and 5×10^6 m^3/s, respectively.

The total northward and southward VTs through Section S4 are 22.7×10^6 and 18.7×10^6 m^3/s, respectively, with a net northward VT of 4.0×10^6 m^3/s. Southwest off the Philippines, the total eastward and westward VTs through Section E4 are 8.3×10^6 and 11.5×10^6 m^3/s, respectively, with a

net westward VT of 3.2×10^6 m^3/s.

(4) Circulation in the southeastern SCS. There is mainly a cyclonic circulation system (C3) in the southeastern SCS. C3 has a large scope extending from southwest to northeast. It is not strong, but covers the eastern parts of Sections S1, S2 and S3, and the southern parts of Sections E6 and E4 as well, with a center at about (115°E, 8°N). C3 is shown in fig. 6 as cyclonic in general circulation, in which the stream functions are integrated vertically in the whole layer. However, the flow pattern in the upper layer is different from that in the deep layer. Velocity distribution at Section S2 (figure omitted) shows an anticyclonic flow above 150 m level and a cyclonic flow below 200 m level over the Nansha Trough, even though their velocities are quite small. This circulation system has its special thermal structure, as mentioned above, there is a warm water center at 100 m level (fig. 2(a)) but a cold center at both 700 and 1 200 m levels (fig. 2(b), (c)) in that area. Fang et al.[3] have reported a circulation structure of anticyclonic flow in the upper layer and cyclonic flow in the lower layer in September 1994, but they are located a little north to the Nansha Islands. Over the Nansha Trough, an anticyclonic flow dominates both the upper and lower layers [3].

As mentioned above, both eddies W2 and C3 cover Sections S1, S2 and S3, and cold eddy C2 also covers Section S3. We will discuss the VTs through Sections S1, S2 and S3 as follows. The total northward and southward VTs through Section S3 are 31.3×10^6 and 30.5×10^6 m^3/s, respectively. The net northward VT through Section S3 is 0.8×10^6 m^3/s, i.e. the northward and southward VTs through Section S3 are almost balanced in the water exchange between the northern and southern SCSs. In addition, most of the VT through Section S3 is converged in the western SCS east off Vietnam, where the warm eddy W2 is located. In the southern SCS, the total northeastward and southwestward VTs through Section S2 are 24.4×10^6 and 23.9×10^6 m^3/s, respectively, with a net northeastward VT of 0.5×10^6 m^3/s, i.e. the VTs through Section S2 in the two directions are almost balanced. The total northeastward and southwestward VTs through Section S1 are 16.6×10^6 and 19.2×10^6 m^3/s, respectively, with a net southwestward VT of 2.6×10^6 m^3/s. From the distribution of VTs, it can also be seen that the currents and eddies in the western SCS are stronger than those in the eastern SCS, except the intrusion of the Kuroshio branch near the Bashi Channel.

In summary, the circulation in the SCS has a characteristic of multi-eddy structure: cyclonic eddies C1, C2 and C3, anticyclonic eddies W1, W2 and W3, which can be seen from the distributions of stream function (fig. 6), water temperature (fig. 2) and ADCP currents (fig. 4). It is interesting that some larger scale eddies contain several small eddies, e.g. the anticyclonic eddy W3 includes two smaller eddies W3-1 and W3-2 west off the Philippines. From the variation of the thermal fields, it is obvious that these eddies have a close relationship with the variation of baroclinic fields.

3 Summary

Based on the hydrographical and meteorological data obtained by R/V *Xiangyanghong No.14* in the SCS in the summer of 1998, the current velocity and VT are calculated by the modified inverse model. The circulation and mesoscale eddies in the SCS are discussed and analyzed by comparing the calculated results with temperature distribution and ADCP data. The following results are obtained.

The most important feature of the circulation in the northeastern SCS is that a branch of the Kuroshio intrudes into the SCS with a small volume transport. The branch of the Kuroshio can affect the SCS circulation in an area west to 117°E and south to 18°N. It flows through the Bashi Channel and towards the southwest off the Taiwan Island anticyclonically, and it does not intrude into the inner SCS.

The northern SCS is dominated mainly by a cyclonic circulation system with two cold eddies. There is a wide scope of cold water in the upper layer, while the scope becomes smaller and almost substituted by the two warm eddies in the deep layer.

The central and southwestern SCSs are mainly occupied by anticyclonic circulation systems, including the strong anticyclonic eddy southeast off Vietnam (W2), anticyclonic eddy near Zhongsha Islands (W1), and the anticyclonic circulation system west off the Philippines. There is a stronger cyclonic eddy (C2) between the two anticyclonic eddies W1 and W2.

In the southeastern SCS, there is a large scope of cyclonic circulation extending in the SW-NE

direction.

There is a “multi-eddy phenomenon” in the SCS, and a larger eddy contains several smaller eddies. Besides, the circulation pattern in the upper layer is different from that in the lower layer.

In general, both the currents and eddies in the western SCS are stronger than those in the eastern part except those near the Bashi Channel.

Acknowledgements This paper is greatly improved by the reviewers. This work was supported by the Major State Basic Research Program (Grant No. G1999043802).

References

1. Xu, X., Qiu, H., Chen, H., The general descriptions of the horizontal circulation in the South China Sea, Proceedings of the 1980 Symposium on Hydrometeology of the Chinese Society of Oceanology and Limnology (in Chinese), Beijing: Science Press, 1982, 137—145.
2. Villanoy, C. L., Udarbe, M. J. B., The circulation in the eastern South China Sea during May 1993, The Philippine Scientist: Special Issue, 1995, 128—142.
3. Fang, W., Guo, Z., Huang, Y., Observational study of the circulation in the southern South China Sea, Chinese Science Bulletin, 1998, 43(11): 898.
4. Chou, D., Density circulation of the central water of South China Sea, Report of Comprehensive Survey in the Central South China Sea (1) (in Chinese), Beijing: Science Press, 1982, 129—139.
5. Huang, Q., Ocean currents in Nansha Area, Proceedings of Physical Oceanography in Nansha Area (Ⅰ) (in Chinese), Beijing: China Ocean Press, 1994, 10—27.
6. Zeng, Q., Li, F., Ji, Z., Computation of monthly circulation in the South China Sea, Scientia Atmospherica Sinica (in Chinese), 1989, 13(2): 127.
7. Liu. X., Su. J., A reduced model of the circulation in the South China Sea, Oceanologia et Limnologia Sinica (in Chinese), 1992, 23(2): 167.
8. Su, J., Xu, J., Cai, S. et al., Circulation and eddies in the South China Sea, Onset and Evolution of the South China Sea Monsoon and Its Interaction With the Ocean (eds. Ding, Y., Li, C.) (in Chinese), Beijing: China Meteorological Press, 1999, 272—279.
9. Chern, C. S., Wang, J., A numerical study of the summertime flow around the Luzon Strait, J. Oceanogr., 1998, 54: 53.
10. Chu, P. C., Chen, Y., Lu, S., Wind driven South China Sea deep basin warm-core/cold core eddies, J. Oceanogr., 1998, 54: 347.
11. Takano, K., Harashima, A., Namba, T., A numerical simulation of the circulation in the South China Sea——Preliminary results, Acta Oceanographica Taiwan, 1998, 37(2): 165.
12. Wu, C. R., Shaw, P. T., Chao, S. Y., Seasonal and interannual variations in the velocity field of the South China Sea, J. Oceanogr., 1998, 54: 361.
13. Cai, S., Wang, W., Three-dimensional numerical simulation of South China Sea circulation in winter and summer, Acta Oceanologica Sinica (in Chinese), 1999, 21(2): 27.
14. Yuan, Y., Su, J., Pan, Z., Volume and heat transports of the Kuroshio in the East China Sea in 1989, La Mer, 1992, 30: 251.
15. Yuan, Y., Kaneko, A., Su, J. et al., The Kuroshio east of Taiwan and in the East China Sea and the currents east of Ryukyu Islands during early summer of 1996, J. Oceanogr., 1998, 54: 217.
16. Fiadeiro, M. E., Veronis, G., On the determination of absolute velocities in the ocean, Journal of Marine Research, 1982, 40(Suppl.): 159.
17. Yuan, Y., Liu, Y., Su, J. et al., Kuroshio east of Taiwan Island and in the East China Sea in winter of 1997, Oceanography in China (12) (in Chinese), Beijing: China Ocean Press, 2000, 11—20.
18. Guan, B., A review of study on the South China Sea Warm Current, Oceanologia et Limnologia Sinica (in Chinese), 1998, 29(3): 322.

(Received March 20, 2000; accepted April 10, 2000)